EnvironmentAsia
The international journal published by the Thai Society of Higher Education Institutes on Environment

Available online at www.tshe.org/EA
EnvironmentAsia 1 (2009) 41-48

Enhancement of Catalytic Performance of MCM-41 Synthesized with Rice Husk Silica by Addition of Titanium Dioxide for Photodegradation of Alachlor

Surachai Artkla [a,b,c], Wonyong Choi [c] and Jatuporn Wittayakun [a,b]

[a] *Material Chemistry Research Unit, School of Chemistry, Suranaree University of Technology, Nakhon Ratchasima, 30000, Thailand*
[b] *National Center of Excellence for Environmental and Hazardous Waste Management, Faculty of Engineering, Thammasat University, 12120, Thailand*
[c] *School of Environmental Science and Engineering, Pohang University of Science and Technology, Pohang, 790-784, Korea*

Abstract

Photocatalytic degradation of alachlor, a herbicide, in water on both bare TiO_2 and TiO_2 supported on mesoporous material, marked as TiO_2/RH-MCM-41 were studied. The RH-MCM-41 support was synthesized from rice husk silica and other reagents by hydrothermal method. The required amount of titanium precursor (TiO_2 P25 Degussa) to give 10-60% was mixed with RH-MCM-41 and calcined at 300 °C for 6 h. The catalytic activities of TiO_2 and TiO_2/RH-MCM-41 for alachlor degradation were performed under UV radiation with wavelength of 300 nm. The ratio of catalyst weight to volume of alachlor solution was 1 g/L and all products were characterized by high performance liquid chromatograph. The reaction equilibrium was established in 30 min. in deionized water without adjusting the solution pH. The TiO_2/RH-MCM-41 could adsorb alachlor more than the bare TiO_2 (namely, 17% vs. 5%) and the photocatalytic activity of alachlor degration on all TiO_2/RH-MCM-41s was higher than that on the bare TiO_2. By comparison per weight of TiO_2, the 10%TiO_2/RH-MCM-41 gave the highest alachlor conversion of 100% after 20 min. while 1% bare TiO_2 showed conversion of 95%.

***Keywords*:** alachlor; RH-MCM-41; photodegradation; titanium dioxide; TiO_2

1. Introduction

Alachlor (2-chloro-2′,6′-diethyl-N-(methoxymethyl) acetanilide), one of variety of herbicides, is used in agricultural lands. It can contaminate water and raises various problems including carcinogenesis, neurotoxicity and effect on reproduction and cell development (Burrows *et al*., 2002). Because alachlor is stable-to-natural decomposition, its degradation either by conventional, biological or physical method is not effective (Bhattacharyya *et al.*, 2004; Li *et al*, 2007). A recent method to decompose it is by advanced oxidation processes (AOPs) which involve the generation of reactive species such as hydroxyl radical ($HO^{\bullet}$) to break down organic compounds (Konstantinou and Albanis, 2004). Titanium dioxide (TiO_2) is a photocatalyst that can generate the $HO^{\bullet}$ for such purpose. Unfortunately, the use of TiO_2 is limited by structure and morphological aspects, for example, the bare TiO_2 can be deactivated by electron-hole recombination (Carp *et al*., 2004). Recent researches have been concerning on both degradation and adsorption of alachlor on many solid catalysts for example, Wong and Chu (2003) investigated photocatalytic degradation of alachlor by bare suspension of TiO_2 with hydrogen peroxide (H_2O_2). They showed the effect of UV light power, suitable dose of H_2O_2 for reaction and product distribution. Moreover, adsorption of alachlor on different clays was also done by Sanchez-Martin *et al*., (2006). Because kinetics and adsorption of alachlor on mesoporous materials were rarely concerned, this study investigated an improvement in catalytic activity of TiO_2 by dispersing it on RH-MCM-41 of which the surface composed of hydroxyl groups. Hole-electron recombination could be suppressed and active species could be easily transferred to degrade pollutants.

2. Materials and Methods

2.1. Preparation of RH-MCM-41and TiO_2/RH-MCM-41

RH-MCM-41 was synthesized with rice husk silica, prepared as in (Wittayakun *et al*., 2008) and cetyltrimethylammonium bromide (CTABr) in NaOH solution (3.33 M) with the gel molar ratio of 1.0SiO_2 : 3.0NaOH : 0.25CTABr : 180H_2O. The mixture pH was adjusted to 11.5 and the gel was crystallized at 100 °C for 24 h, filtered, dried, and calcined at 540 °C for 6 h.

The TiO_2/RH-MCM-41 was prepared by physically mixing of TiO_2 and RH-MCM-41. A desired amount of TiO_2 was added to slurry of RH-MCM-14 in deionized water under continuous stirring during a 2-hour period. The mixture was washed several times to remove Na^+ ions with de-ionized water, dried and calcined at 300 °C for 6 h. The prepared TiO_2/RH-MCM-41 catalysts contained 10, 20, 40 and 60% of TiO_2.

2.2. Catalyst characterizations

The crystalline phase of bare TiO_2 and TiO_2/RH-MCM-41 were analyzed using X-ray powder diffraction (XRD: Rigaku Model D/Max III) with CuK_α radiation. The X-ray was generated with a current of 40 mA and a potential of 40 kV. The catalyst powder (0.20 g) was pressed in a sample holder and scanned from 10 to 80 degrees (2θ) in steps of 0.05 degrees per minute. The powder patterns of all samples were recorded in similar procedure with the same amount of material, so that the intensity of the peak height (100) could be compared.

Physical characteristics of the sample were determined by N_2 adsorption-desorption isotherm at -196 °C for relative pressure from 10^{-2} to 0.99 on an AUTOSORB-1 analyzer. Before measurement, sample was degassed with heat at 250 °C for 3 h. The BET surface area was obtained from the N_2 adsorption data in the relative pressure range of 0.02 to 0.2. The pore volumes was calculated from the desorption branches if the isotherm using Barrett-Joyner-Halenda (BJH) method.

The optical absorption spectra of bare TiO_2 and TiO_2/RH-MCM-41 powders were recorded using a Shimadzu UV-Vis spectrophotometer equipped with a diffuse reflectance attachment (Shimadzu ISR-2200). All sample powders were diluted with $BaSO_4$ (TiO_2:$BaSO_4$ = 1:17) and referenced to $BaSO_4$. In order to understand electric potential in the interfacial double layer at the location of the slipping plane versus a point in the bulk fluid away from the interface of bare TiO_2, RH-MCM-41 and TiO_2/RH-MCM-41, the electrokinetic potential or zeta potential in colloidal systems of these materials was measured. In the procedure, the electrophoretic mobilities of bare TiO_2, RH-MCM-41 and TiO_2/RH-MCM-41 particles were suspended in water with the concentration of 0.5 g/L and measured to determine their zeta potentials as a function of pH by using an electrophoretic light scattering spectrophotometer (ELS 8000, Otsuka) equipped with a He–Ne laser and a thermostated flat board cell.

2.3. Adsorption isotherm determination of alachlor on catalysts

Adsorption behavior of alachlor was investigated by mixing each catalyst powder in 30 mL alachlor (70-100 μM) at weight per volume ratio of 1 g/L. The solution pH was adjusted by HNO_3 and LiOH standard solutions before the mixture was sonicated for 30 s and stirred in the dark for 30 min. Sample aliquots of 1 mL were collected at appropriate time intervals, filtered through 0.45-μm PTFE filters (Millipore) and analyzed by a high performance liquid chromatograph (HPLC: Agilent 1100 series) equipped with a diode array to determine alachlor adsorption.

2.4. Photocatalytic degradation of alachlor

All experiments were carried out in a pyrex reactor (33 mL) with a quartz window. The catalyst powder was well suspended at 1.0 g/L in 30 mL alachlor (100 μM) by sonicating for 30 s. The initial pH (pH_i) of the suspension was adjusted with HNO_3 or LiOH standard solutions. A Xe-arc lamp (300 W, Oriel) was used as the illumination. Sample aliquots of 1 mL were collected at appropriate time intervals and filtered through 0.45-μm PTFE filters (Millipore). Alachlor and its mineralized products were analyzed using a high performance liquid chromatograph (HPLC: Agilent 1100 series) equipped with a diode array.

Effect of loading TiO_2 on RH-MCM-41 was studied by varying TiO_2 loading from 10 to 60 wt% as well as comparing with bare TiO_2. The synergic effect of RH-MCM-41 support was performed and the catalytic activities in the dark and under UV irradiation were also compared. The catalytic performance of TiO_2/RH-MCM-41 was studied at various concentrations of alachlor in the range of 70-100 μM. In addition, the reaction rate was monitored with the decrease of alachlor concentration. Then reaction order was obtained from the plot between time and alachlor concentration. Finally, pH influencing reaction was carried out in the range of 2 to 8. The results were shown in the relationship between pH versus conversion and reaction rate.

3. Results and discussion

3.1. Catalyst characterizations

XRD spectra of the bare TiO_2 and all TiO_2/RH-MCM-41 are shown in Fig.1. The TiO_2 which was used as purchased composed of anatase and rutile with 80:20 ratios. The intensities of TiO_2 increased when the loading of TiO_2 on RH-MCM-41 was increased. There was no phase transformation from anatase TiO_2 to rutile TiO_2 because all the TiO_2/RH-MCM-41 catalysts were calcined at 300 °C, lower than the phase transformation temperature which is

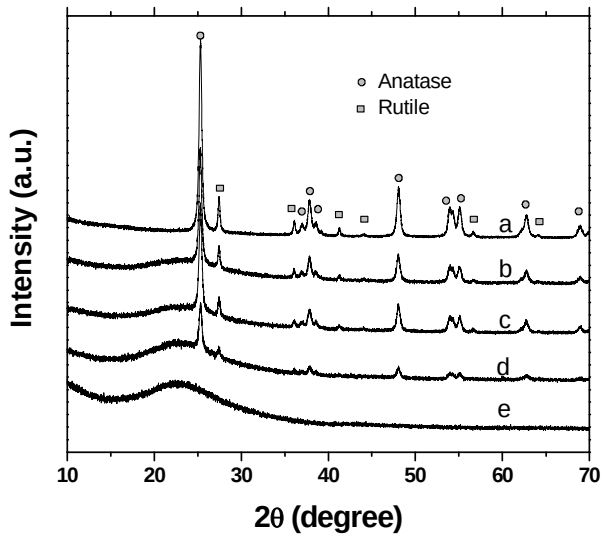

Figure 1. XRD spectra of bare TiO_2 and TiO_2/RH-MCM-41; (a) TiO_2 (b) 60%TiO_2/RH-MCM-41 (c) 40% TiO_2/RH-MCM-41 (d) 10% TiO_2/RH-MCM-41 (e) RH-MCM-41.

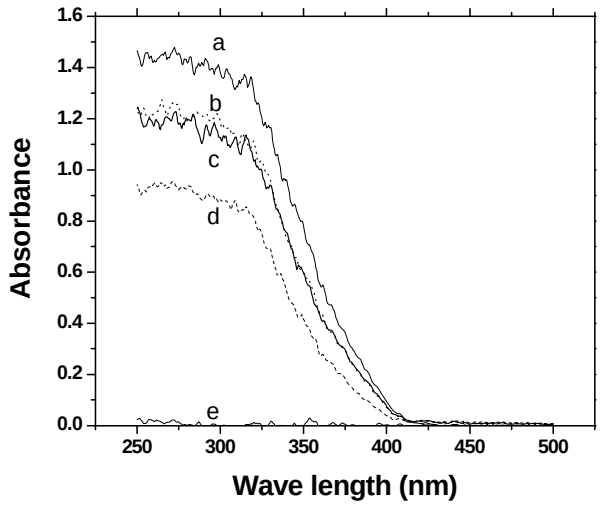

Figure 2. UV-visible diffuse reflectance spectra of bare TiO_2 and TiO_2/RH-MCM-41; (a) TiO_2 (b) 60%TiO_2/RH-MCM-41 (c) 40% TiO_2/RH-MCM-41 (d) 10% TiO_2/RH-MCM-41 (e) RH-MCM-41.

625 °C (Vohra *et al*., 2005). In this case, anatase TiO_2 was available for active site for photocatalytic degradation of alachlor.

Surface areas of all catalysts are shown in Table 1. The surface area of TiO_2/RH-MCM-41 decreased with loading amount of TiO_2 indicating that TiO_2 covered some part of surface area of RH-MCM-41. However, 60 wt% of TiO_2 loading still possessed higher surface area than the bare TiO_2 implied that there were more active sites on TiO_2/RH-MCM-41 due to the dispersion on RH-MCM-41. In addition, the pore volumes of all TiO_2/RH-MCM-41s were higher than 160 cm^3/g implying that the adsorption capacities of TiO_2/RH-MCM-41s were greater than that of the bare TiO_2. Activities of all catalysts were expected to rely on adsorptive properties between reagent and active site. If the adsorption was performed properly, reaction would also proceed well.

In Fig. 2, the effect of RH-MCM-41 on the adsorption of TiO_2 was investigated. It was expected that the modification of TiO_2 by dispersing on RH-MCM-41 would reduce its band gap energy, less than 3.2 eV. If this phenomenon occurred, electrons in valence band would be easily excited to conduction band. Consequently, $HO^{\bullet}$ could be easily produced for photocatalytic degradation and the degradation would proceed faster. However, the results from DR-UV showed that the blue shift of absorption edge in the diffuse reflectance of UV spectra of any TiO_2/RH-MCM-41 was not observed. In addition, the UV absorption of all catalysts depended on the amount of TiO_2. RH-MCM-41 but did not enhance bare TiO_2 to adsorb more UV-light indicating that band gap of bare TiO_2 did not change. When comparing the adsorption of 40%RH-MCM-41 and 60%RH-MCM-41, the adsorptive intensities were almost the same implying that 60 wt% TiO_2 was an excess load for dispersion on the surface of RH-MCM-41. Thus, the TiO_2 amount of 40 wt% or less was suitable to produce good dispersion on RH-MCM-41 and the photodegradation of alachlor was expected to improve.

Table 1. BET surface area and volume adsorption at STP of TiO_2 and TiO_2/RH-MCM-41

Materials	S_{BET} (m^2/g)	Volume adsorbed (cm^3/g STP)
TiO_2 (P25)	50.0	-
10% TiO_2/RH-MCM-41	757.9	204.3
20% TiO_2/RH-MCM-41	727.1	198.5
40% TiO_2/RH-MCM-41	662.1	167.8
60% TiO_2/RH-MCM-41	590.0	160.6

The zeta potential of RH-MCM-41, TiO_2/RH-MCM-41 and bare TiO_2 in Fig. 3 were at 2.25, 2.90 and 6.75 mV, respectively. The trend indicated that positively charged surface increased in order of TiO_2 > TiO_2/RH-MCM-41 > RH-MCM-41. From this result, TiO_2 was expected to dominate in charge interaction to aromatic ring of alachlor. However, charge interaction was negligible in this study because adsorption mode was predominated by Freundlich isotherm which was the adsorption between non-charged compound and charged surface of solid catalysts. The adsorption characteristics of alachlor on RH-MCM-41 were compared in Figs. 4(a-b).

3.2. Adsorption isotherm of alachlor

Figs. 4(a-b), show adsorption of alachlor on catalysts studied in the dark condition by stirring the mix-

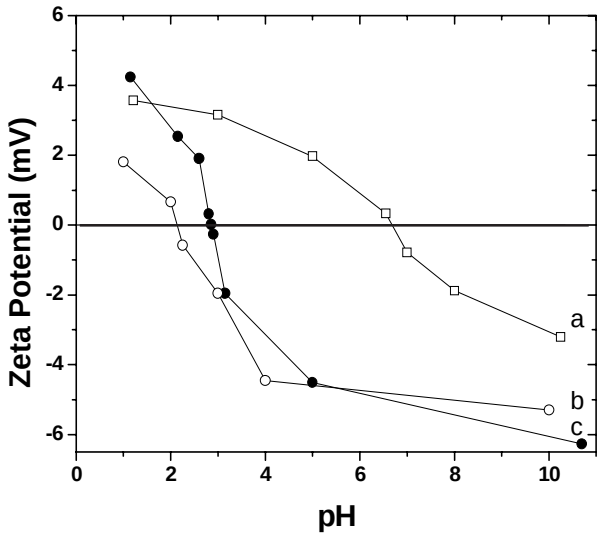

Figure 3. Zeta potential of TiO_2 and TiO_2/RH-MCM-41; (a) TiO_2 (b) RH-MCM-41 (c) 10%TiO_2/RH-MCM-41.

ture of alachlor and catalyst and sampled after 0.5 h. Several adsorptive parameters were concerned including the equilibrium concentration of alachlor in solution, the amount of adsorbed alachlor on the catalyst at the equilibrium concentration, the maximum adsorption amount and the apparent adsorption equilibrium concentration. The results were described in both Langmuir and Freundlich isotherms in equation (1) and (2), respectively.

$$\frac{C_e}{q_e} = \frac{C_e}{q_{max}} + \frac{1}{K_{ad} \times q_{max}} \quad (1)$$

$$Log(q_e) = Log(K) + \frac{1}{n} Log(C_e) \quad (2)$$

Where

C_e = equilibrium concentration of alachlor in solution (mg/L)

q_e = amount of adsorbed alachlor on the catalyst at the equilibrium concentration (mg/g)

q_{max} = maximum adsorption amount of alachlor (mg/g)

K_{ad} = apparent adsorption equilibrium concentration $(mg/L)^{-1}$

K = adsorption capacity constant $(mg/L)^{-1}$

n = adsorption layer of alachlor

The relationship between C_e/q_e and C_e were plotted and it did not obey Langmuir model because a linear relationship was not obtained [see Fig. 4(a)]. This indicated that surface-charge interaction between alachlor and TiO_2/RH-MCM-41 was not only chemisorption but also physisorption. Thus, Freundlich model was studied and the results are shown in Fig. 4(b). From equation (2), a straight line with the slope and R^2 of 0.67 and 0.98, respectively, was obtained. A number of adsorption layers (n) from the relationship between n and slope were 1.50 confirming the previous reasons that adsorption between organic or inorganic compounds on adsorbent should be multi-layers.

3.3. Photodegradation of alachlor on bare TiO_2 and TiO_2/RH-MCM-41

3.3.1. Effect of TiO_2 loading on RH-MCM-41 to photodegradation

In order to obtain the optimal amount of TiO_2 added on RH-MCM-41, various amounts of TiO_2, 10,

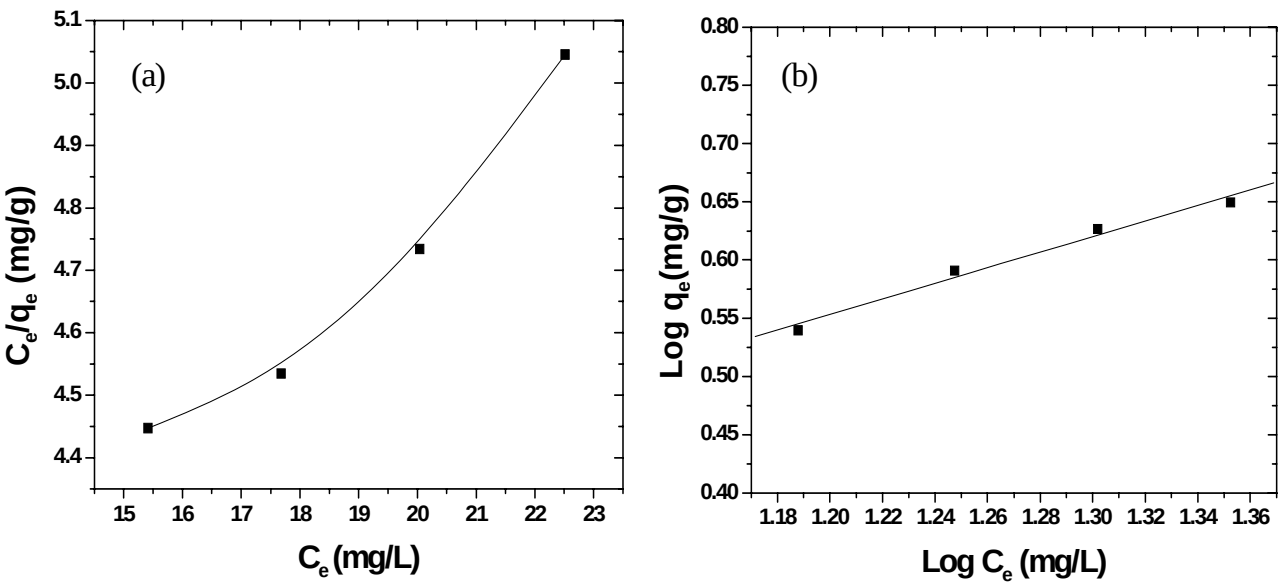

Figure 4. Adsorption of alachlor on TiO_2/RH-MCM-41; (a) Langmuir isotherm (b) Freundlich isotherm; [TiO_2/RH-MCM-41] = 1 g/L, pH = 4, [alachlor] = 80 μM, UV light = 300 nm.

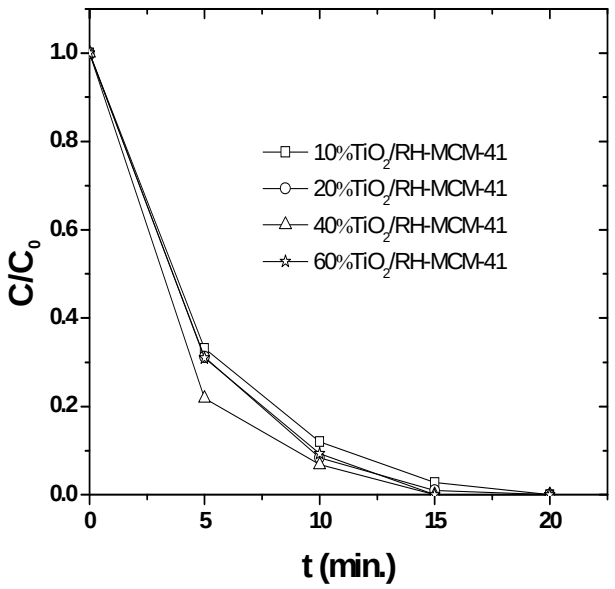

Figure 5. Photocatalytic degradation of alachlor on various TiO_2/RH-MCM-41s; [TiO_2/RH-MCM-41] = 1 g/L, pH = 4, [alachlor] = 80 μM, UV light = 300 nm.

20, 40 and 60 wt%, were used. Their performances for photodegradation in Fig. 5 showed that the degradation rate was not different significantly with different TiO_2 loading. All catalysts showed 100% conversion of alachlor around 15-20 min. when compared the ration of conversion to amount of TiO_2 loading, 10 wt% was worth to use. Thus, results suggested an optimal 10%TiO_2/RH-MCM-41 to achieve most effective degradation of alachlor.

3.3.2. Synergic effect of support and UV light

The comparison between the photocatalytic degradation of alachlor on bare TiO_2 and on TiO_2/RH-MCM-41 is exhibited on Fig. 6. In this study, the catalyst concentration and the power of UV light were fixed at 1 g/L and 300 nm because Vohra *et al*., (2005) had proven that the suitable amount of TiO_2 for photoreaction was in the range of 0.5-1 wt. According to Fig. 6, TiO_2/RH-MCM-41 in the dark did not show any activity while the blank reaction (without catalyst) with sole UV light showed about 40% change in alachlor concentration implying that UV light is necessary for this reaction. Without UV light, there was no energy to generate $HO^{\bullet}$ radical in TiO_2/RH-MCM-41. In addition, alachlor could automatically degrade but reaction time to obtain complete conversion would be too long. In the case of RH-MCM-41 with UV irradiation, the degradation rate was slightly greater than that in the blank and 50% conversion of alachlor was achieved after 30 min. This showed synergic effect of support due to the face that RH-MCM-41 had brϕnsted acid site for adsorption and degradation of alachlor. For TiO_2/RH-MCM-41 and bare TiO_2, 100% conversion of alachlor was achieved on 20 and 30 min. for TiO_2/RH-MCM-41 and bare TiO_2, respectively. This indicated the enhancement of photocatalytic degradation of alachlor by dispersing of TiO_2 on RH-MCM-41 support because RH-MCM-41 provided higher OH density on the surface (Vohra *et al*., 2005). There are two reasons to support this hypothesis. First, the surface hydroxyl group play important role in direct participation in the reaction mechanism by trapping photo-generated holes that reach catalyst surface producing reactive surface $HO^{\bullet}$ radical (Hoffmann *et al*., 1995). Second, surface hydroxyl group can change the adsorption of reactant molecule by both serving as active site for pollutant adsorption and covering the site on TiO_2 where electrons are trapped (Maira *et al*., 2000).

3.3.3. Effect of alachlor concentration

Fig. 7 shows the effect of alachlor concentration. The alachlor concentration of 80 μM possessed the highest degradation rate. For the concentration higher than 80 μM, the certain loading of TiO_2/RH-MCM-41 produced a certain amount of hydroxyl radical which may not be sufficient for all alachlor molecules. For the lower concentration, alachlor molecules may adsorb more strongly on the surface and had lower degradation rate (Wang *et al*., 2008). Further information, the initial rate of reaction was exhibited in Fig. 8. The degradation rate agreed with the results in Fig. 7 that the reaction proceeded rapidly when the alachlor concentration was 80 μM.

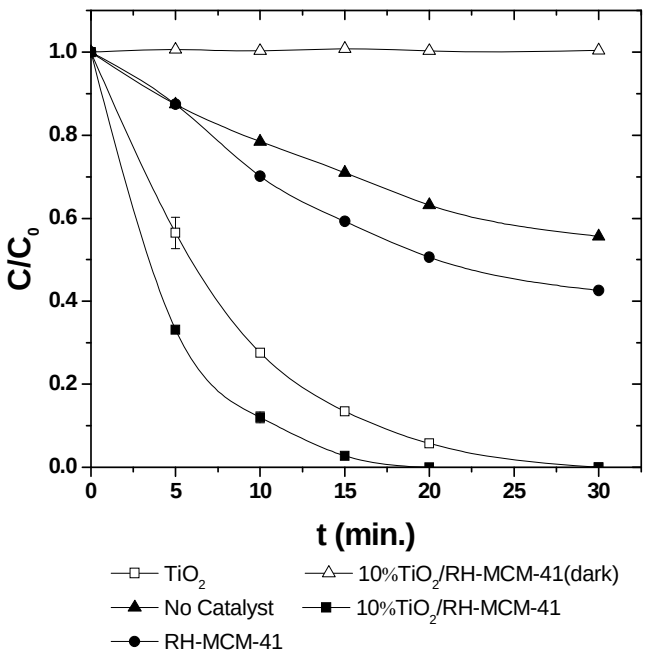

Figure 6. Photocatalytic degradation of alachlor on bare TiO_2, TiO_2/RH-MCM-41, dark control TiO_2/RH-MCM-41 and RH-MCM-41; [TiO_2/RH-MCM-41] = 1 g/L, pH = 4, [alachlor] = 80 μM, UV light = 300 nm.

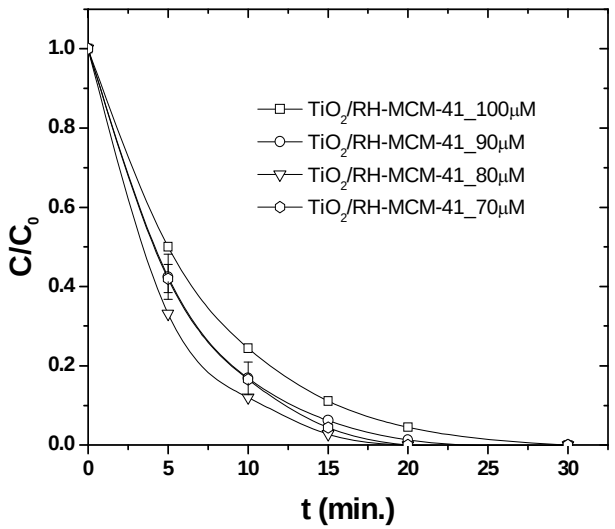

Figure 7. Effect of concentration influencing photocatalytic degradation of alachlor; [TiO_2/RH-MCM-41] = 1 g/L, pH = 4, UV light = 300 nm.

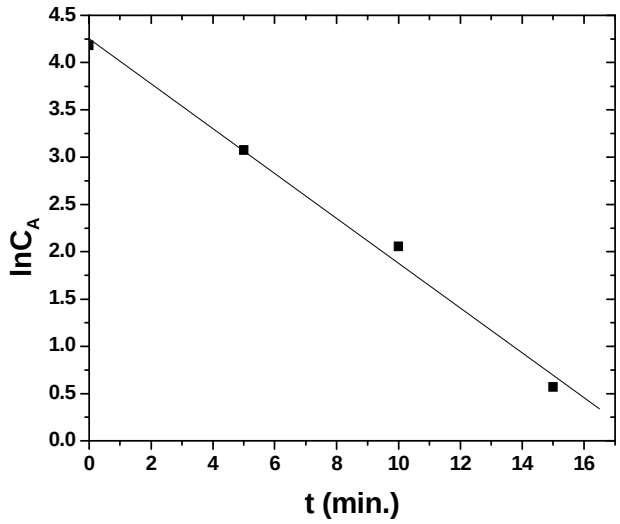

Figure 9. pseudo-first order plot from photocatalytic degradation of alachlor; [TiO_2/RH-MCM-41] = 1 g/L, pH = 4, [alachlor] = 80 μM, UV light = 300 nm.

3.3.4. Kinetics of reaction

The kinetics of alachlor degradation was investigated to determine the reaction order. In Fig. 9, the plot between $\ln C_A$ versus time gave a straight line with slope and R^2 of 0.23 and 0.9926, respectively corresponding to the mathematic formula below:

$$\ln(C_A) = -kt + \ln C_{A_0} \qquad (3)$$

From the equation, rate constant (k) of alachlor degradation was 0.23 min^{-1}. This result implied that photocatalytic degradation alachlor obeyed the pseudo-first order model as expressed by equation (3).

3.3.5. Effect of pH

Fig. 10 exhibits the effect of pH to photocatalytic degradation of alachlor. Eventhough, pH change did not affect the charge of alachlor molecule, surface charge was really sensitive to the pH change. In order to understand a role of pH, we already reported surface properties of TiO_2/RH-MCM-41 and bare TiO_2 by studying zeta potential in Fig. 3. Corresponding to the previous result, photocatalytic degradation of alachlor reached the highest efficiency at pH4 because the surface charge of catalyst at this pH was nearly zero. The adsorption between neutral alachlor and surface functional group should be compromised

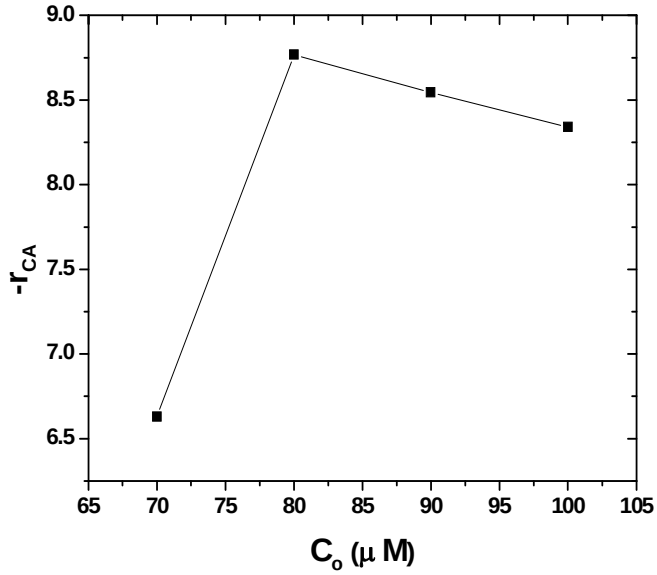

Figure 8. Initial degradation rate of alachlor by differential method; [TiO_2/RH-MCM-41] = 1 g/L, pH = 4, UV light = 300 nm.

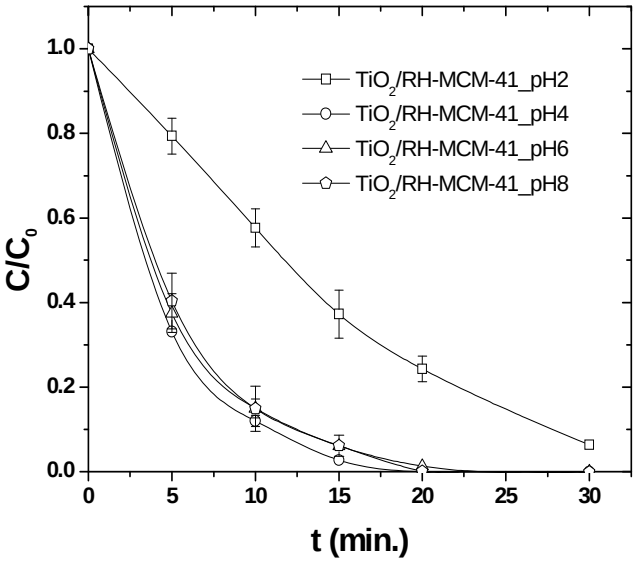

Figure 10. Effect of pH influencing photocatalytic degradation of alachlor; [TiO_2/RH-MCM-41] = 1 g/L, [alachlor] = 80 μM, UV light = 300 nm.

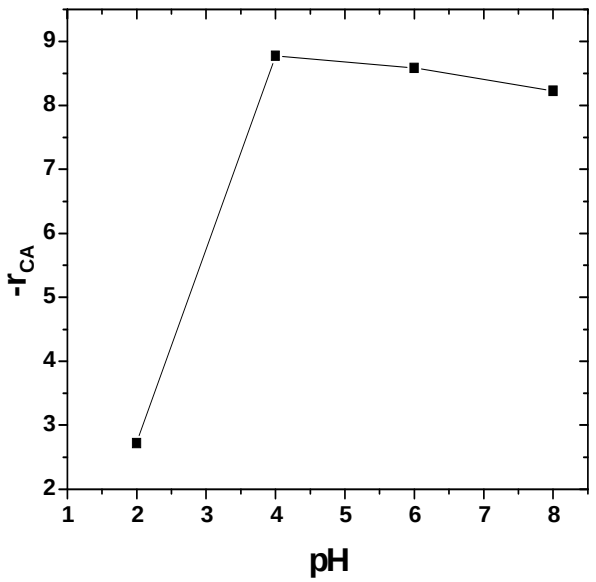

Figure 11. Initial degradation rate of alachlor influencing by pH solution; [TiO_2/RH-MCM-41] = 1 g/L, [alachlor] = 80 μM, UV light = 300 nm.

in this condition. Finally, Fig. 11 also confirmed that the degradation rate was highest when the solution pH was 4. At lower pH, the surface charge was positive and the interaction between alachlor and catalyst surface was unfavorable resulting in lower degradation. At the pH higher than 4, the degradation rate decreased gradually even though the surface had negative charge. In this case, the reaction did not only occur on active site of the catalyst but also on the bulk solution. This can refer to Kim and Choi's study (Kim and Choi, 2002) which reported that the hydroxyl radical could be produced on both catalyst surface and bulk solution.

4. Conclusions

The photocatalytic performance of TiO_2 could be enhanced by dispersing on mesoporous materials, RH-MCM-41, prepared form rice husk silica. The morphology and crystalinity of TiO_2 did not change after modification. The reaction was strongly dependent on pH solution because surface functional group of solid catalysts was sensitive to pH change. The neutral surface dominated reaction by playing an important role for adsorption of a neutral alachlor molecule. TiO_2/RH-MCM-41 was more preferable for photocatalytic degradation than the bare TiO_2 since it possessed higher OH groups.

Acknowledgements

A scholarship for S. Artkla and research funding are from Suranaree University of Technology and National Synchrotron Research Center (Grant 2-2548/PS01).

References

Bhattacharyya A, Kawi S, Ray MB. Photocatalytic degradation of orange II by TiO_2 catalysts supported on adsorbents. Catalysis Today 2004; 98: 431-39.

Burrows HD, Canle LM, Santaballa JA, Steenken S. Reaction pathways and mechanisms of photodegradation of pesticides. Journal of Photochemistry and Photobiology B: Biology 2002; 67: 71-108.

Carp O, Huisman CL, Reller A. Photoinduced reactivity of titanium dioxide. Progress in Solid state Chemistry 2004; 32: 33-177.

Hoffmann MR, Martin ST, Choi W, Bahnemann DW. Environmental applications of semiconductor photocatalysis. Chemical Reviews 1995; 95: 69-96.

Kim S, Choi W. Kinetics and mechanisms of photocatalytic degradation of $(CH_3)_nNH_{4-n}^+$ ($0 \le n \le 4$) in TiO_2 suspension: The role of OH radicals. Environmental Science and Technology 2002; 36: 2019-25.

Konstantinou IK, Albanis TA. TiO_2-assisted photocatalytic degradation of azo dyes in aqueous solution: kinetic and mechanistic investigations: A review. Applied Catalysis B: Environmental 2004; 49: 1-14.

Li G, Zhao XS, Ray MB. Advanced oxidation of orange II using TiO_2 supported on porous adsorbents: The role of pH, H_2O_2 and O_3. Separation and Purification Technology 2007; 55: 91-97.

Maira A, Yeung KL, Yan CY, Yue PL, Chan CK. Size Effects in gas-phase photo-oxidation of trichloroethylene using nanometer-sized TiO_2 catalysts. Journal of Catalysis 2000; 192: 185-96.

Sanchez-Martin MJ, Rodriguez-Cruz MS, Andrades MS, Sanchez-Camazano M. Efficiency of different clay minerals modified with a cationic surfactant in the adsorption of pesticides: Influence of clay type and pesticide hydrophobicity. Applied Clay Science 2006; 31: 216- 28.

Vohra MS, Lee J, Choi W. Enhanced photocatalytic degradation of tetramethylammonium on silica-loaded titania. Journal of Applied Electrochemistry 2005; 35:757-63.

Wang H, Nui J, Long X, He Y. Sonophotocatalytic degradation of methyl orange by nano-sized Ag/TiO_2 particles in aqueous solutions. Ultrasonics Sonochemistry 2008; 15: 386-92.

Wittayakun J, Khemthong P, Prayoonpokarach S. Synthesis and characterization of zeolite NaY from rice husk silica. Korean Journal of Chemical Engineering 2008; 24: 861-64.

Wong CC, Chu W. The hydrogen peroxide-assisted photocatalytic degradation of alachlor in TiO_2 suspensions. Environmental Science and Technology 2003; 37: 2310-16.

Received 19 October 2008
Accepted 7 December 2008

Correspondence to
Dr. Jatuporn Wittayakun
School of Chemistry, Institute of Science
Suranaree University of Technology
111 University Ave., Muang District,
Nakhon Ratchasima, 30000
Thailand
Fax: 66-(0)44-224-185
Tel: 66-(0)44-224-256
Website:http://www.sut.ac.th/Science/chemistry/jatuporn.htm